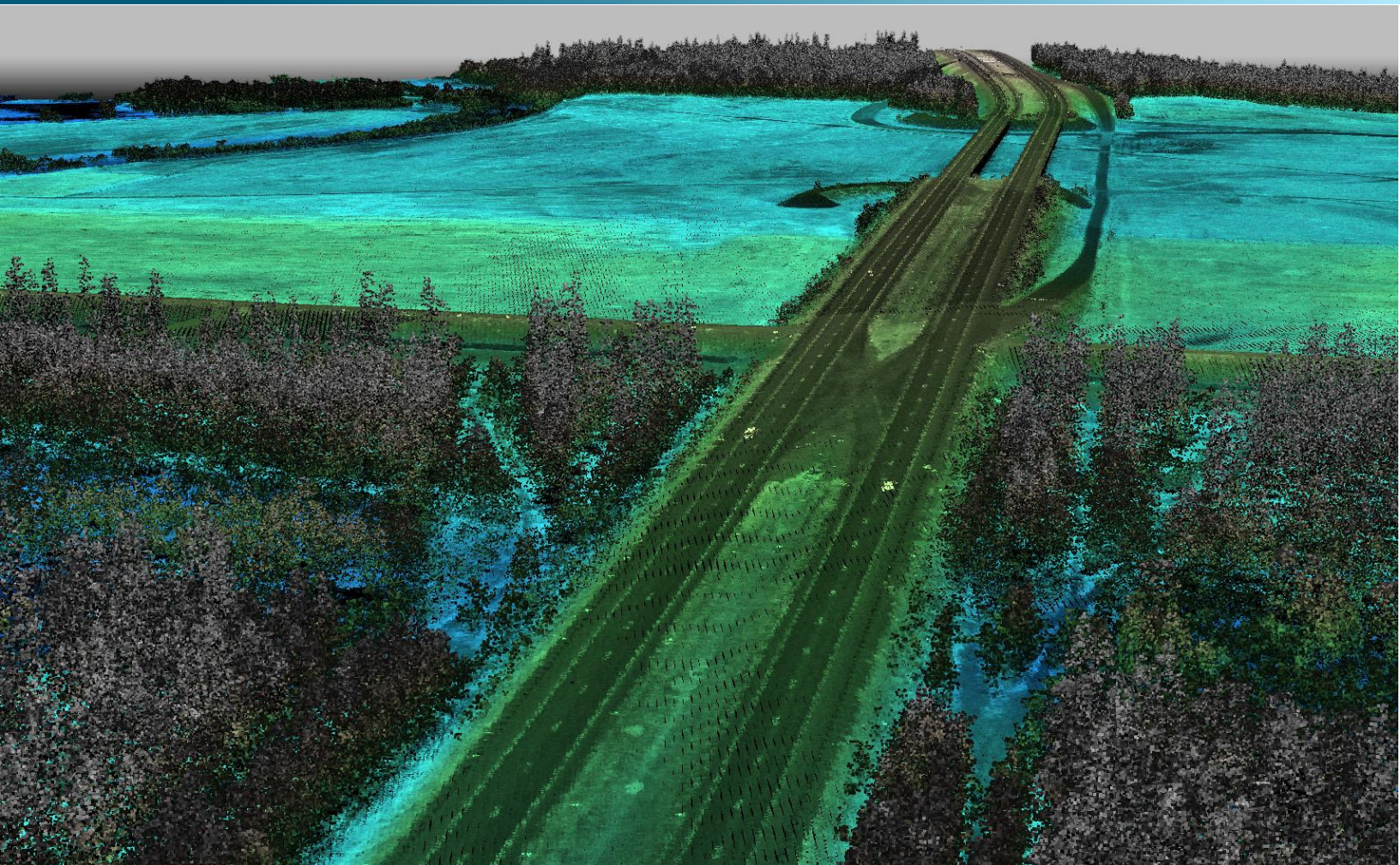




June 9, 2016



Chena River Lakes LiDAR

Technical Data Report



Stanley Ponsness
DOWL LLC
4041 B St
Anchorage, AK 99503-5999
PH: 907-562-2000



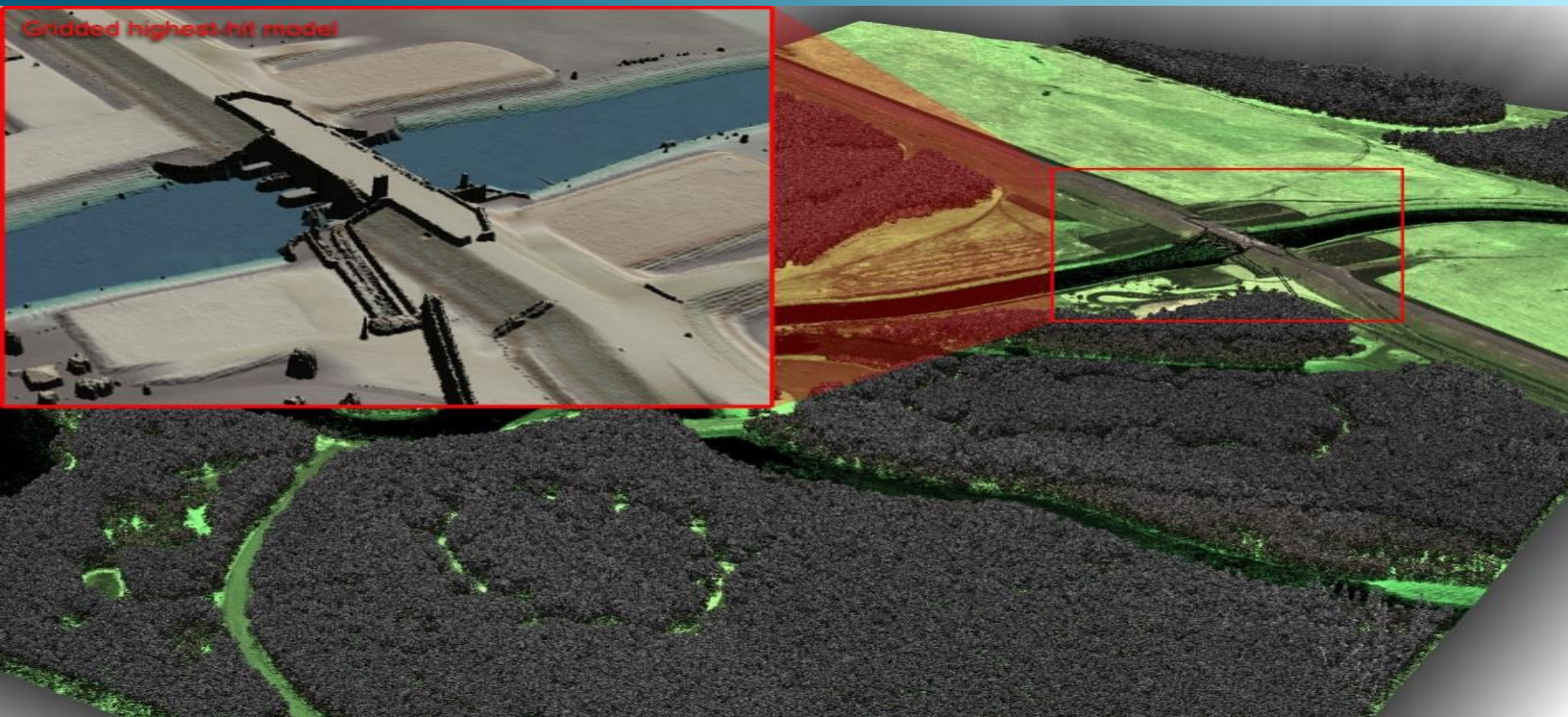
QSI Anchorage Office
2014 Merrill Field Drive
Anchorage, AK 99501
PH: 907-272-4495

TABLE OF CONTENTS

INTRODUCTION	5
Deliverable Products	6
ACQUISITION	8
Planning.....	8
Airborne LiDAR Survey	9
Ground Control.....	11
Monumentation	11
Ground Survey Points (GSPs).....	11
Land Cover Class	12
PROCESSING	14
LiDAR Data.....	14
Feature Extraction.....	16
Contours	16
RESULTS & DISCUSSION.....	17
LiDAR Density	17
LiDAR Accuracy Assessments	21
LiDAR Absolute Accuracy.....	21
LiDAR Supplemental and Consolidated Vertical Accuracies.....	23
LiDAR Relative Vertical Accuracy	26
GLOSSARY	27
APPENDIX A - ACCURACY CONTROLS	28

Cover Photo: A view looking towards the Richardson Highway Bridge in the southwestern portion of the Chena River Lakes AOI. The image was created from the LiDAR bare earth model overlaid with the above-ground point cloud.

INTRODUCTION



In early 2016, Quantum Spatial (QSI) was contracted by DOWL to collect Light Detection and Ranging (LiDAR) data in the spring of 2016 for the Chena River Lakes site in Alaska. Data were collected to aid DOWL in assessing the topographic and geophysical properties of the study area and to support engineering and mapping endeavors.

This report accompanies the delivered LiDAR data and documents contract specifications, data acquisition procedures, processing methods, and analysis of the final dataset including LiDAR accuracy and density. Acquisition dates and acreage are shown in Table 1, a complete list of contracted deliverables provided to DOWL is shown in Table 2, and the project extent is shown in Figure 1.

Table 1: Acquisition dates, acreage, and data types collected on the Chena River Lakes site

Project Site	Contracted Acres	Buffered Acres	Acquisition Dates	Data Type
Chena River Lakes	21,475	22,746	05/01/2016	LiDAR

Introduction photo: This photo shows the Moose Creek Dam in the western portion of the Chena River Lakes AOI. The main image was created from the LiDAR bare earth model overlaid with the above-ground point cloud and the inset image was created from the LiDAR highest hit model, colored by elevation.

Deliverable Products

Table 2: Products delivered to DOWL for the Chena River Lakes site

Chena River Lakes Products	
Projection: Alaska State Plane Zone 3	
Horizontal Datum: NAD83 (NSRS2007)	
Vertical Datum: NAVD88 (GEOID06)	
Units: US Survey Feet	
Points	LAS v 1.2 <ul style="list-style-type: none">• All Returns• Ground Returns
Rasters	3.0 Foot ESRI Grids <ul style="list-style-type: none">• Bare Earth Model• Bare Earth Model Clipped to Water's Edge Breaklines• Highest Hit Model 1.5 Foot GeoTiffs <ul style="list-style-type: none">• Intensity Images
Vectors	Shapefiles (*.shp) <ul style="list-style-type: none">• Site Boundary• LiDAR Tile Index• Smooth Best Estimate Trajectory (SBETs)• Flightlines• Water's Edge Breaklines Geodatabase (*.gdb) <ul style="list-style-type: none">• Contours (1 ft) AutoCAD (*.dxf) <ul style="list-style-type: none">• Smooth Best Estimate Trajectory (SBETs)• Flightline Index

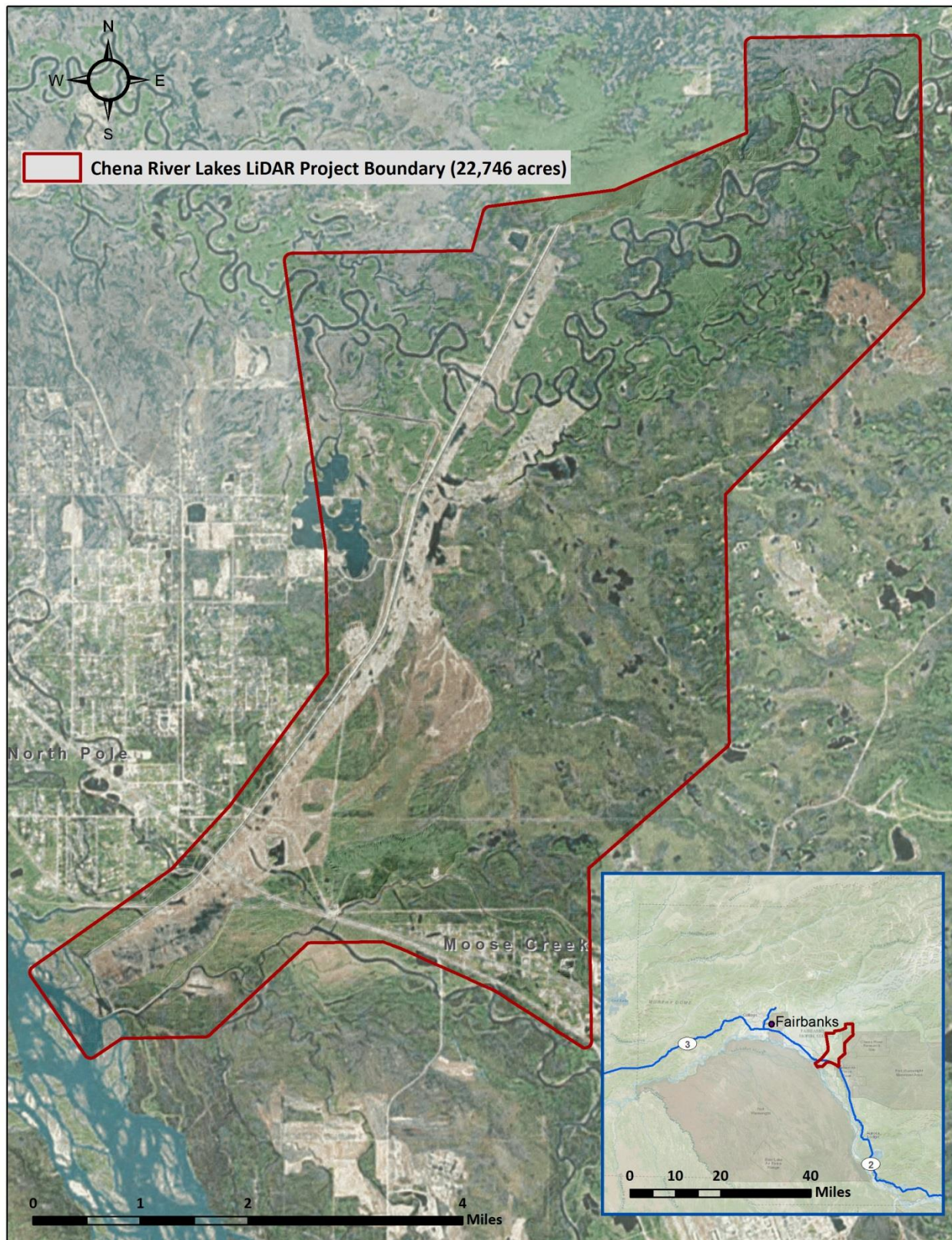


Figure 1: Location map of the Chena River Lakes site in Alaska

ACQUISITION

QSI's Cessna Caravan



Planning

In preparation for data collection, QSI reviewed the project area and developed a specialized flight plan to ensure complete coverage of the Chena River Lakes LiDAR study area at the target point density of ≥ 12.0 points/ m^2 (1.11 points/ ft^2). Acquisition parameters including orientation relative to terrain, flight altitude, pulse rate, scan angle, and ground speed were adapted to optimize flight paths and flight times while meeting all contract specifications.

Factors such as satellite constellation availability and weather windows must be considered during the planning stage. Any weather hazards or conditions affecting the flights were continuously monitored due to their potential impact on the daily success of airborne and ground operations. In addition, logistical considerations including private property access and potential air space restrictions were reviewed.

Airborne LiDAR Survey

The LiDAR survey was accomplished using a Leica ALS80 system mounted in a Cessna Caravan. Table 3 summarizes the settings used to yield an average pulse density of ≥ 12 pulses/m² over the Chena River Lakes project area. The Leica ALS80 laser system can record unlimited range measurements (returns) per pulse. It is not uncommon for some types of surfaces (e.g., dense vegetation or water) to return fewer pulses to the LiDAR sensor than the laser originally emitted. The discrepancy between first return and overall delivered density will vary depending on terrain, land cover, and the prevalence of water bodies. All discernible laser returns were processed for the output dataset.

Table 3: LiDAR specifications and survey settings

LiDAR Survey Settings & Specifications	
Acquisition Dates	May 1, 2016
Aircraft Used	Cessna 208 Caravan
Sensor	Leica ALS80
Survey Altitude (AGL)	1653 m
Swath Width	886 m
Speed	105 knots
Target Pulse Rate	336.4 kHz
Pulse Mode	Multi Pulse in Air (2PiA)
Laser Pulse Diameter	36.3 cm
Laser Power	99.9%
Mirror Scan Rate	47 Hz
Field of View	30°
Beam Wavelength	1064 nm
Frequency of GPS Sampling	2 Hz
Frequency of IMU Sampling	200 Hz
GPS Baselines	≤ 13 nm
GPS PDOP	≤ 3.0
GPS Satellite Constellation	≥ 6
Maximum Returns	Unlimited
Intensity	8-bit
Resolution/Density	Average 12 pulses/m ²
Accuracy	RMSE _Z ≤ 15 cm



Leica ALS80 LiDAR sensor

All areas were surveyed with an opposing flight line side-lap of $\geq 60\%$ ($\geq 100\%$ overlap) in order to reduce laser shadowing and increase surface laser painting. To accurately solve for laser point position (geographic coordinates x, y and z), the positional coordinates of the airborne sensor and the attitude of the aircraft were recorded continuously throughout the LiDAR data collection mission. Position of the aircraft was measured twice per second (2 Hz) by an onboard differential GPS unit, and aircraft attitude was measured 200 times per second (200 Hz) as pitch, roll and yaw (heading) from an onboard inertial measurement unit (IMU). To allow for post-processing correction and calibration, aircraft and sensor position and attitude data are indexed by GPS time.

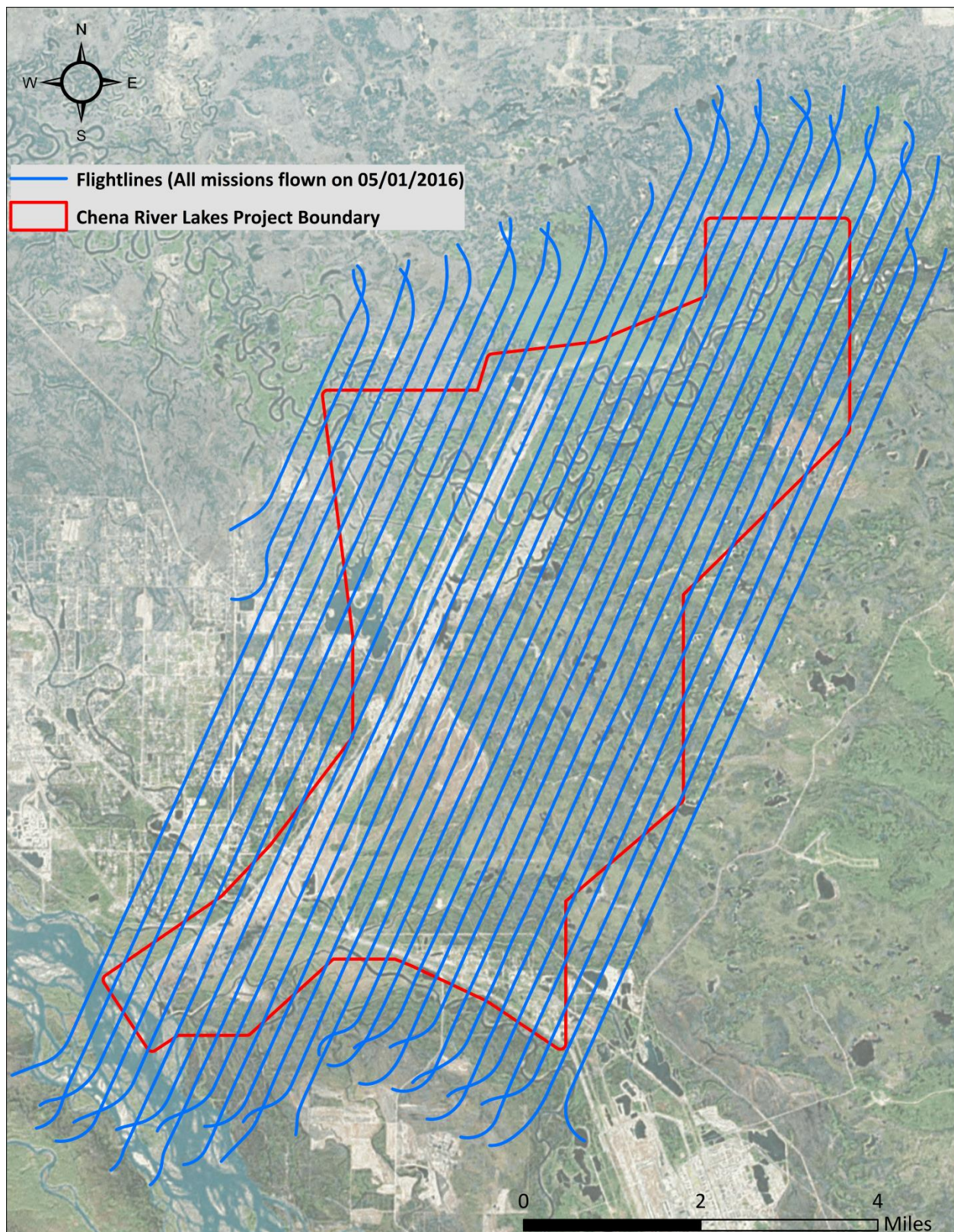


Figure 2: Chena River Lakes Flightline map

Ground Control

Ground control surveys, including monumentation and the collection of ground survey points (GSPs), were conducted by DOWL to support the airborne acquisition. Ground control data were used to geospatially correct the aircraft positional coordinate data and to perform quality assurance checks on final LiDAR data.

Monumentation

QSI used static GNSS data provided by DOWL from base stations set up over three monument locations for the Chena River Lakes LiDAR project (Table 4, Figure 3). All survey data were reviewed by QSI staff upon receipt, and monument positions were verified by processing static GNSS data against nearby Continuously Operating Reference Stations (CORS) using the Online Positioning User Service (OPUS¹).

Table 4: Monuments used for the Chena River Lakes acquisition. Coordinates are on the NAD83 (NSRS2007) datum, epoch 2002.0.

Monument ID	Latitude	Longitude	Ellipsoid (meters)
BUNKER	64° 45' 28.83429"	-147° 13' 16.86350"	167.723
PC 112_12.17	64° 43' 25.09176"	-147° 16' 22.58805"	169.841
GATE	64° 41' 26.19583"	-147° 07' 27.06874"	172.251

Ground Survey Points (GSPs)

Ground survey points were collected by DOWL using real time kinematic survey techniques and supplied to QSI for LiDAR calibration.

¹ OPUS is a free service provided by the National Geodetic Survey to process corrected monument positions. <http://www.ngs.noaa.gov/OPUS>.

Land Cover Class

In addition to ground survey points, land cover class control points were collected and provided by DOWL throughout the study area. Individual accuracies were calculated for each land cover type to assess confidence in the LiDAR-derived ground models across land cover classes. Land cover types and descriptions are shown in Table 5.

Table 5: Land Cover Types and Descriptions

Land cover type	Land cover code	Description
Brush	Brush	Landscape with short vegetation as seen in grazing lands
Gravel	Gravel	Small rocks dominate ground cover with little or no vegetation
Forest	Forest	Tree-dominated landscape where trees are large enough to produce timber
Open Terrain	Open Terrain	Flat, sparsely vegetated terrain
Pavement	Pavement	Flat, man-made surface

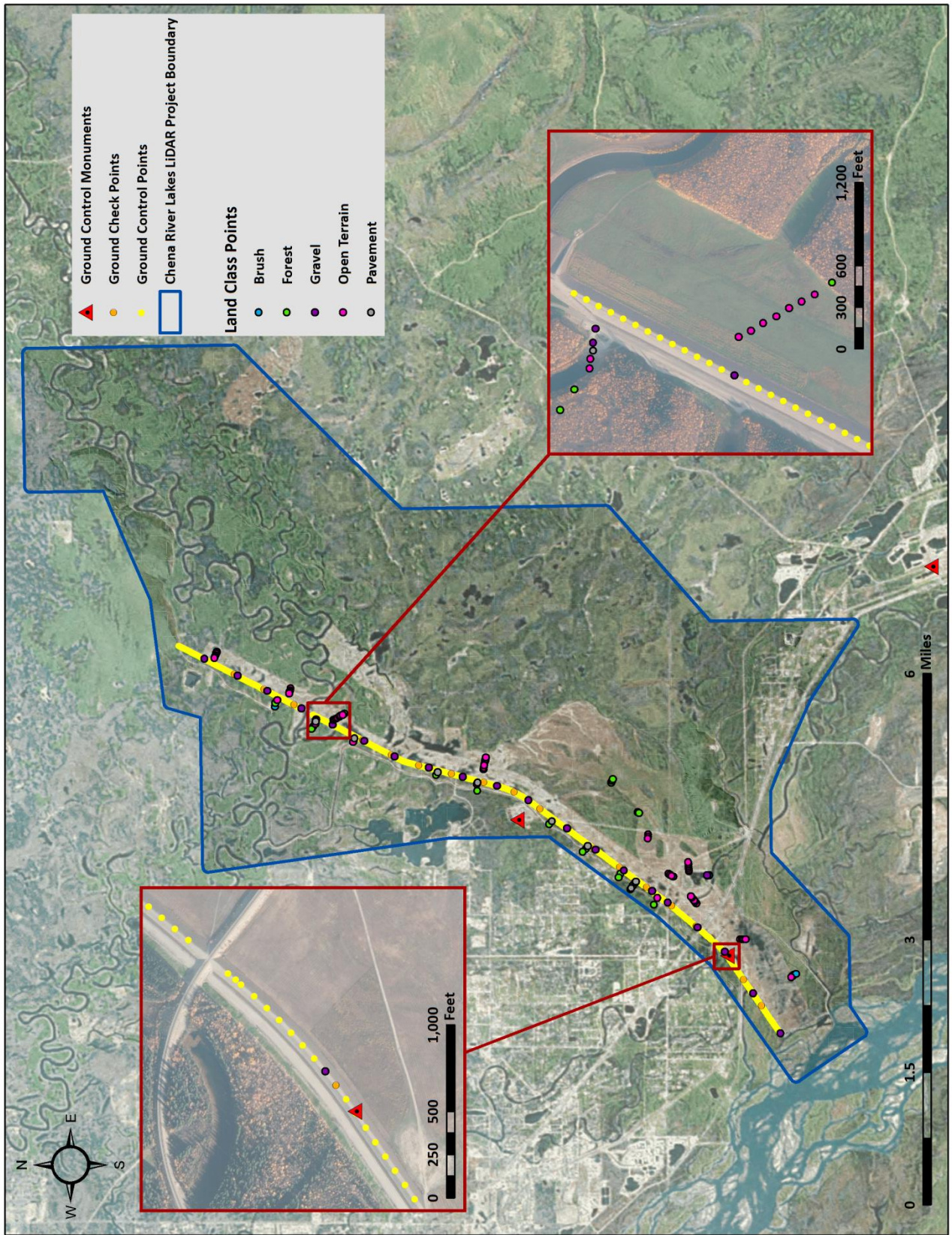
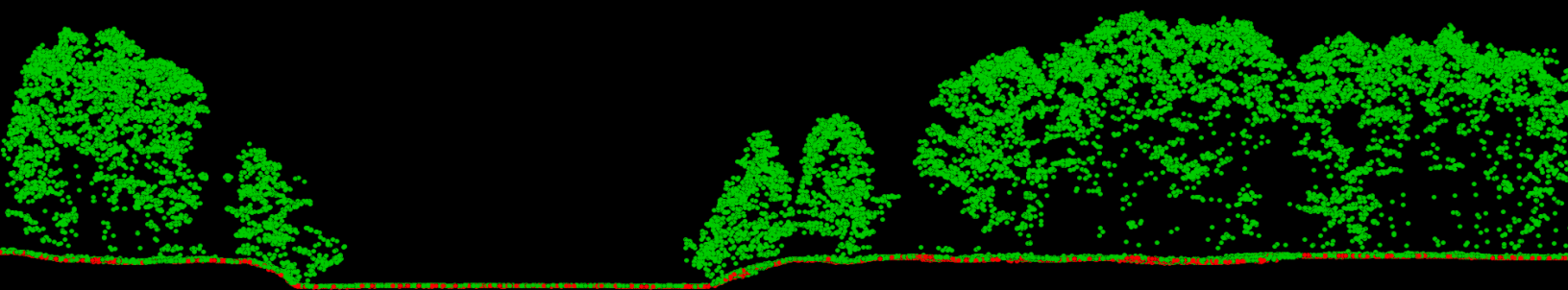


Figure 3: Ground survey location map

PROCESSING

Default
Ground

This 3 meter LiDAR cross section shows a view of the Chena River Lakes landscape, colored by point classification.



LiDAR Data

Upon completion of data acquisition, QSI processing staff initiated a suite of automated and manual techniques to process the data into the requested deliverables. Processing tasks included GPS control computations, smoothed best estimate trajectory (SBET) calculations, kinematic corrections, calculation of laser point position, sensor and data calibration for optimal relative and absolute accuracy, and LiDAR point classification (Table 6). Processing methodologies were tailored for the landscape. Brief descriptions of these tasks are shown in Table 7.

Table 6: ASPRS LAS classification standards applied to the Chena River Lakes dataset

Classification Number	Classification Name	Classification Description
1	Default/Unclassified	Laser returns that are not included in the ground class, composed of vegetation and man-made structures
2	Ground	Laser returns that are determined to be ground using automated and manual cleaning algorithms
7	Noise	Laser returns that are often associated with birds, scattering from reflective surfaces, or artificial points below the ground surface
9	Water	Laser returns that are determined to be water using automated and manual cleaning algorithms

Table 7: LiDAR processing workflow

LiDAR Processing Step	Software Used
Resolve kinematic corrections for aircraft position data using kinematic aircraft GPS and static ground GPS data. Develop a smoothed best estimate of trajectory (SBET) file that blends post-processed aircraft position with sensor head position and attitude recorded throughout the survey.	Waypoint Inertial Explorer v.8.6
Calculate laser point position by associating SBET position to each laser point return time, scan angle, intensity, etc. Create raw laser point cloud data for the entire survey in *.las (ASPRS v. 1.2) format. Convert data to orthometric elevations by applying a geoid06 correction.	Waypoint Inertial Explorer v.8.6 Leica Cloudpro v. 1.2.2
Import raw laser points into manageable blocks to perform manual relative accuracy calibration and filter erroneous points. Classify ground points for individual flight lines.	TerraScan v.16
Using ground classified points per each flight line, test the relative accuracy. Perform automated line-to-line calibrations for system attitude parameters (pitch, roll, heading), mirror flex (scale) and GPS/IMU drift. Calculate calibrations on ground classified points from paired flight lines and apply results to all points in a flight line. Use every flight line for relative accuracy calibration.	TerraMatch v.16
Classify resulting data to ground and other client designated ASPRS classifications (Table 6). Assess statistical absolute accuracy via direct comparisons of ground classified points to ground control survey data.	TerraScan v.16 TerraModeler v.16
Generate bare earth models as triangulated surfaces. Generate highest hit models as a surface expression of all classified points. Export all surface models as ESRI GRIDs at a 3.0 foot pixel resolution.	TerraScan v.16 TerraModeler v.16 ArcMap v. 10.2
Correct intensity values for variability and export intensity images as GeoTIFFs at a 1.5 foot pixel resolution.	LAS Monkey v. 2.2.1 (QSI proprietary) LAS Product Creator v. 1.3 (QSI proprietary) TerraScan v.16 TerraModeler v.16 ArcMap v. 10.2

Feature Extraction

Contours

Contour generation from LiDAR point data required a thinning operation in order to reduce contour sinuosity. The thinning operation reduced point density where topographic change is minimal (i.e., flat surfaces) while preserving resolution where topographic change was present. Model key points were selected from the ground model every 20 feet with the spacing decreased in regions with high surface curvature. Generation of model key points eliminated redundant detail in terrain representation, particularly in areas of low relief, and provided for a more manageable dataset. Contours were produced through TerraModeler by interpolating between the model key points at even elevation increments.

Elevation contour lines were then intersected with ground point density rasters and a confidence field was added to each contour line. Contours which crossed areas of high point density have high confidence levels, while contours which crossed areas of low point density have low confidence levels. Areas with low ground point density are commonly beneath buildings and bridges, in locations with dense vegetation, over water, and in other areas where laser penetration to the ground surface was impeded (Figure 4).

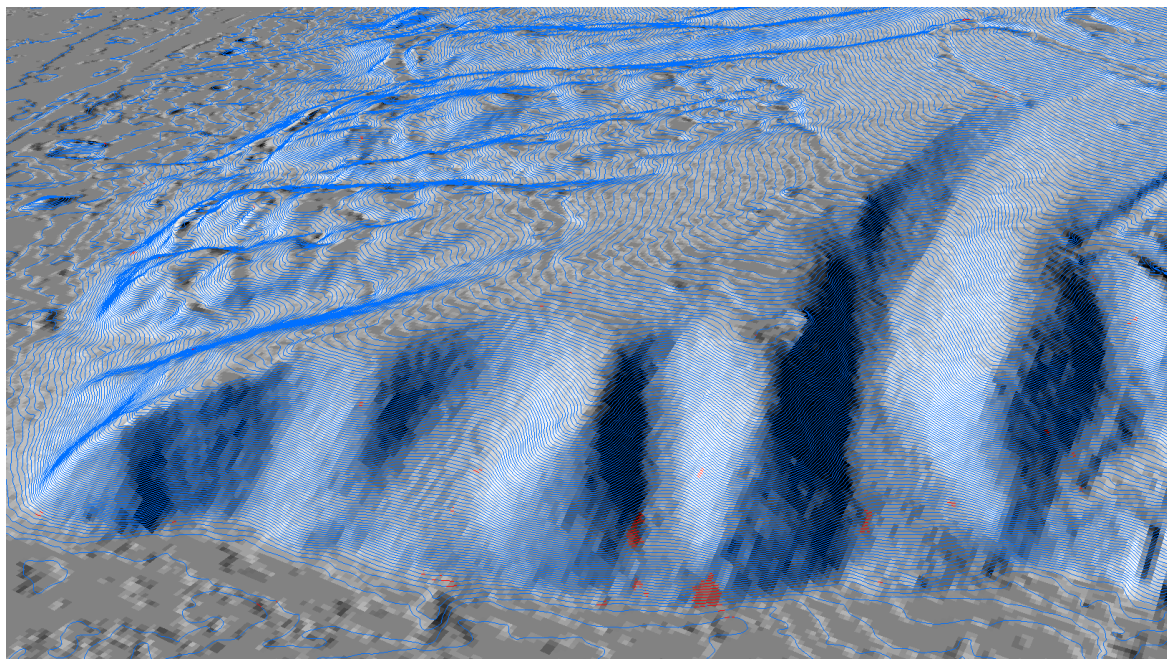
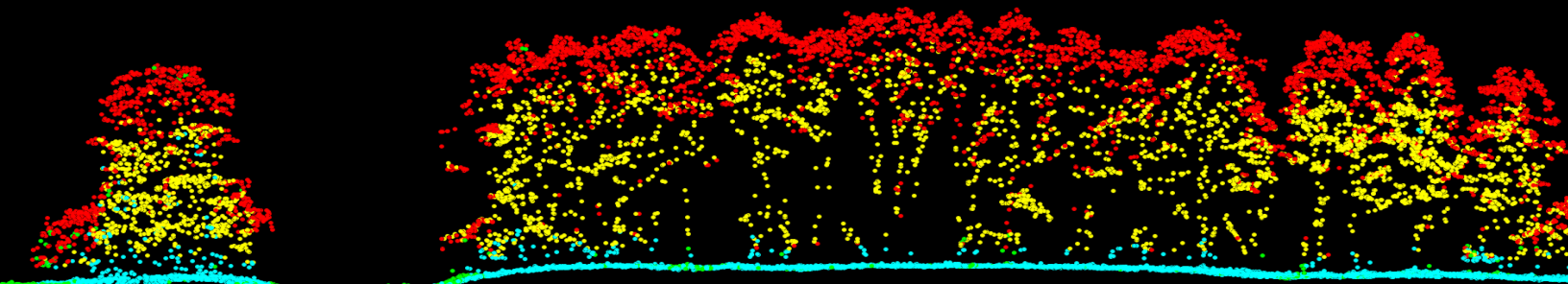


Figure 4: Contours draped over the Chena River Lakes bare earth elevation model. Blue contours represent high confidence while the red contours represent low confidence.

RESULTS & DISCUSSION

Only Echo
First of Many
Intermediate
Last of Many

This 2 meter LiDAR cross section shows a view of vegetation and bare ground in the Chena River Lakes AOI, colored by point laser echo.



LiDAR Density

The acquisition parameters were designed to acquire an average first-return density of ≥ 12.0 points/ m^2 (1.11 points/ ft^2). First return density describes the density of pulses emitted from the laser that return at least one echo to the system. Multiple returns from a single pulse were not considered in first return density analysis. Some types of surfaces (e.g., breaks in terrain, water and steep slopes) may have returned fewer pulses than originally emitted by the laser. First returns typically reflect off the highest feature on the landscape within the footprint of the pulse. In forested or urban areas the highest feature could be a tree, building or power line, while in areas of unobstructed ground, the first return will be the only echo and represents the bare earth surface.

The density of ground-classified LiDAR returns was also analyzed for this project. Terrain character, land cover, and ground surface reflectivity all influenced the density of ground surface returns. In vegetated areas, fewer pulses may penetrate the canopy, resulting in lower ground density.

The average first-return density of LiDAR data for the Chena River Lakes project was 1.31 points/ ft^2 (14.11 points/ m^2) while the average ground classified density was 0.26 points/ ft^2 (2.85 points/ m^2) (Table 8). The statistical and spatial distributions of first return densities and classified ground return densities per $100\text{ m} \times 100\text{ m}$ cell are portrayed in Figure 5 through Figure 8.

Table 8: Average LiDAR point densities

Classification	Point Density
First-Return	1.31 points/ ft^2 14.11 points/ m^2
Ground Classified	0.26 points/ ft^2 2.85 points/ m^2

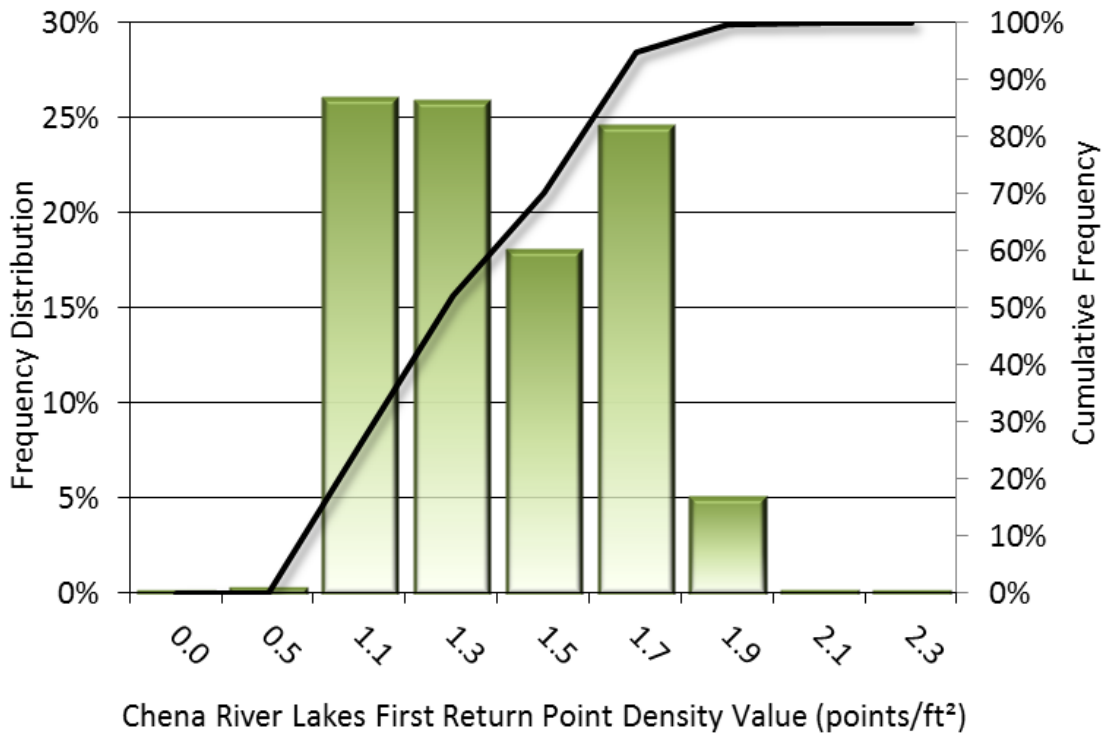


Figure 5: Frequency distribution of first return point density values per 100 x 100 m cell

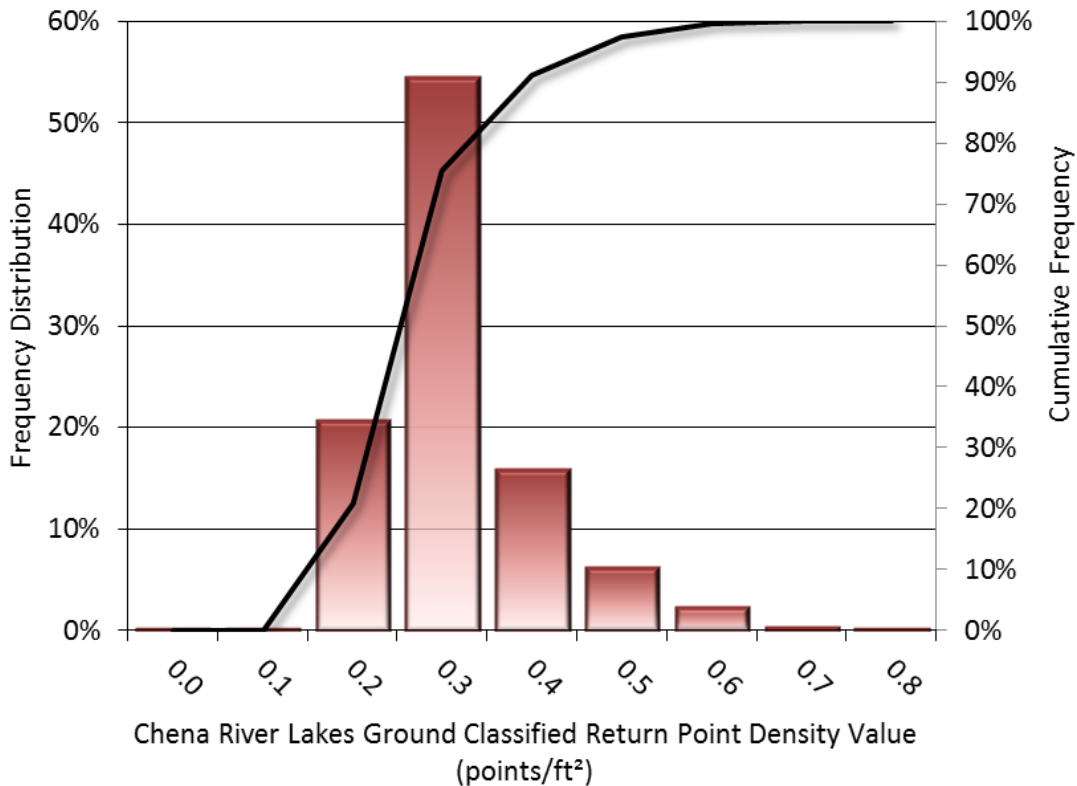


Figure 6: Frequency distribution of ground-classified return point density values per 100 x 100 m cell

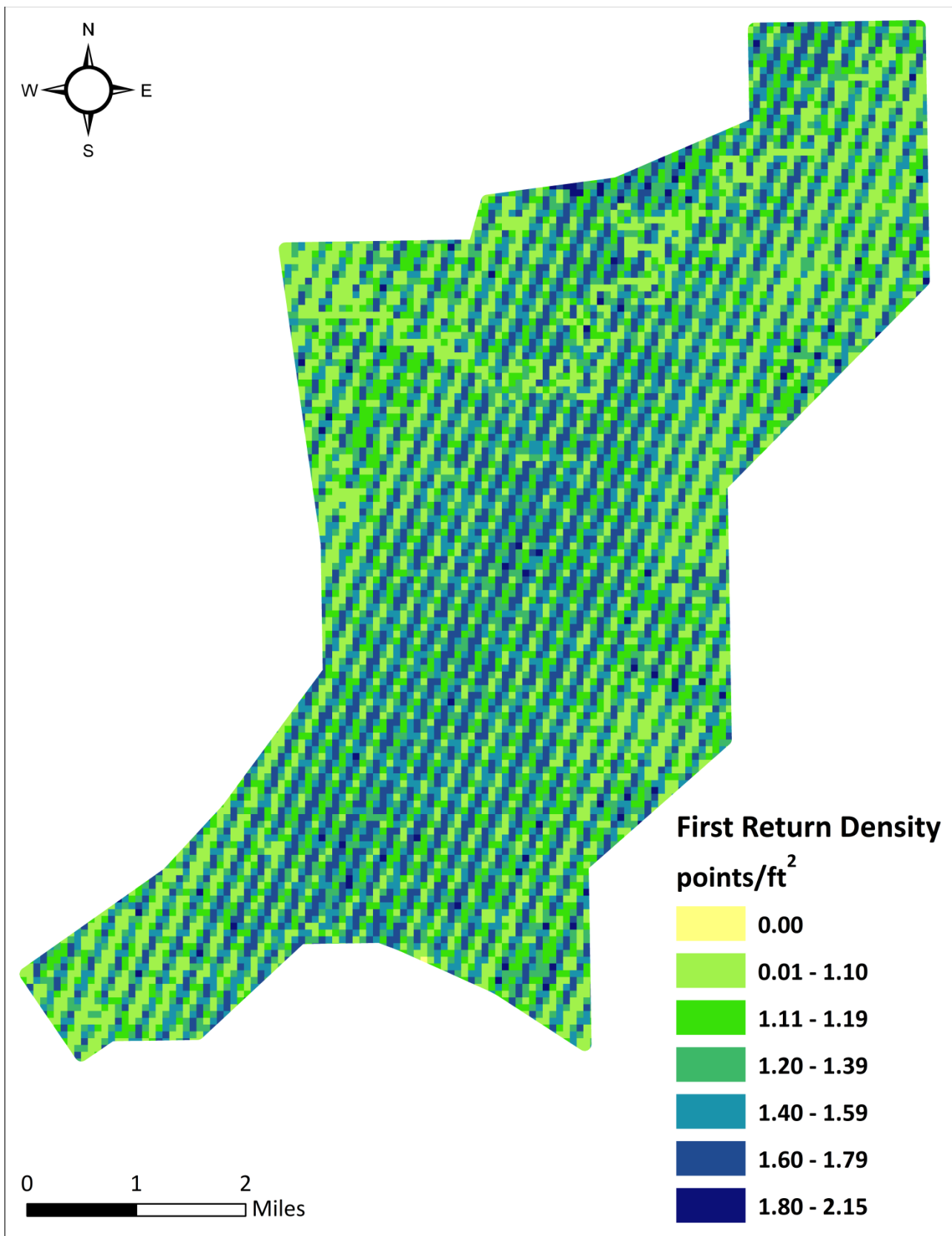


Figure 7: First return point density map for the Chena River Lakes site (100 m x 100 m cells)

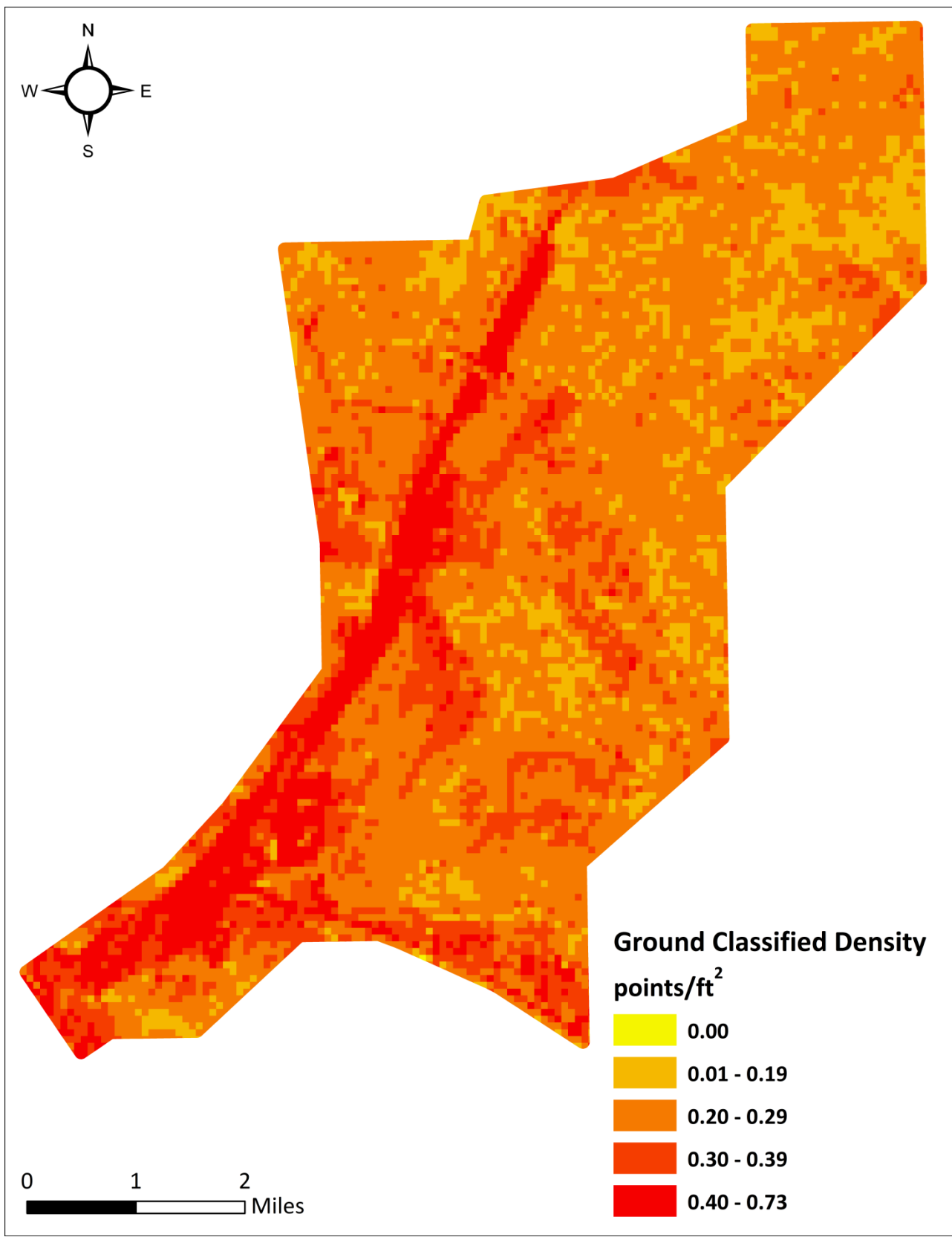


Figure 8: Ground point density map for the Chena River Lakes site (100 m x 100 m cells)

LiDAR Accuracy Assessments

The accuracy of the LiDAR data collection can be described in terms of absolute accuracy (the consistency of the data with external data sources) and relative accuracy (the consistency of the dataset with itself). See Appendix A for further information on sources of error and operational measures used to improve relative accuracy.

LiDAR Absolute Accuracy

Absolute accuracy was assessed using Fundamental Vertical Accuracy (FVA) reporting designed to meet guidelines presented in the FGDC National Standard for Spatial Data Accuracy². FVA compares known ground quality assurance point data collected on open, bare earth surfaces with level slope ($<20^\circ$) to the triangulated surface generated by the LiDAR points. FVA is a measure of the accuracy of LiDAR point data in open areas where the LiDAR system has a high probability of measuring the ground surface and is evaluated at the 95% confidence interval ($1.96 * \text{RMSE}$), as shown in Table 9.

The mean and standard deviation (σ) of divergence of the ground surface model from quality assurance point coordinates are also considered during accuracy assessment. These statistics assume the error for x, y, and z is normally distributed, and therefore the skew and kurtosis of distributions are also considered when evaluating error statistics. For the Chena River Lakes survey, 80 quality assurance points were used for Fundamental Vertical Accuracy (FVA) calculations which resulted in an FVA value of 0.188 feet (0.057 meters) (Figure 9).

The absolute accuracy was also assessed using 416 ground control points. Although these points were used in the calibration and post-processing of the LiDAR point cloud, they may still provide a good indication of the overall accuracy of the LiDAR dataset, and therefore have been provided in Table 9 and Figure 10.

Table 9: Absolute accuracy results

Absolute Accuracy	
	Quality Assurance Points (FVA)
Sample	80 points
FVA ($1.96 * \text{RMSE}$)	0.201 ft 0.061 m
Average	0.049 ft 0.015 m
Median	0.041 ft 0.013 m
RMSE	0.103 ft 0.031 m
Standard Deviation (1σ)	0.091 ft 0.028 m

²Federal Geographic Data Committee, Geospatial Positioning Accuracy Standards (FGDC-STD-007.3-1998). Part 3: National Standard for Spatial Data Accuracy. <http://www.fgdc.gov/standards/projects/FGDC-standards-projects/accuracy/part3/chapter3>

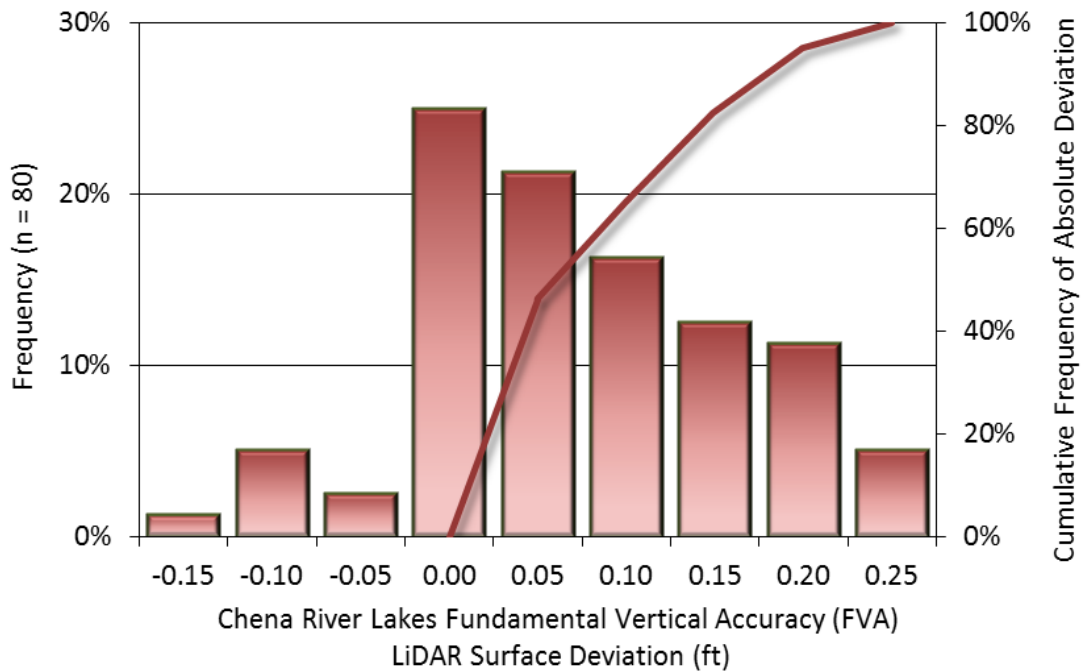


Figure 9: Frequency histogram for LiDAR surface deviation from quality assurance point values (FVA)

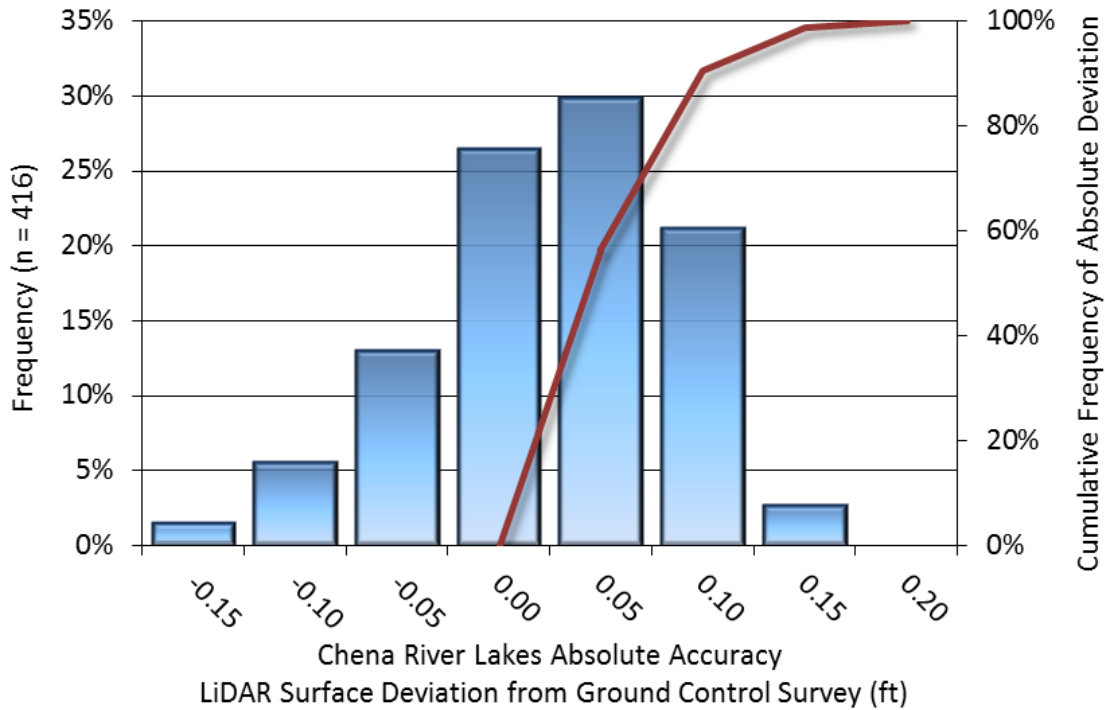


Figure 10: Frequency histogram for LiDAR surface deviation from ground control point values

LiDAR Supplemental and Consolidated Vertical Accuracies

Vertical accuracy was also assessed using Supplemental Vertical Accuracy (SVA) and Consolidated Vertical Accuracy (CVA) reporting. SVA compares known ground check point data within individual land cover class categories to the triangulated ground surface generated by the ground classified LiDAR points while CVA compares known ground check points within all land cover classes. SVA and CVA are evaluated at the 95th percentile, as shown in Table 10 and Figure 11 through Figure 14.

Table 10: Supplemental and Consolidated Vertical Accuracies for the Chena River Lakes Project

Supplemental and Consolidated Vertical Accuracies				
Land Cover Class	SVA			CVA
Sample	Brush	Gravel	Forest	All Land Cover Classes
Average Dz	10 points 0.231 ft 0.071 m	24 points 0.031 ft 0.010 m	20 points 0.112 ft 0.034 m	134 points 0.069 ft 0.021 m
Median	0.205 ft 0.063 m	0.041 ft 0.013 m	0.107 ft 0.033 m	0.066 ft 0.020 m
RMSE	0.264 ft 0.080 m	0.076 ft 0.023 m	0.204 ft 0.062 m	0.137 ft 0.042 m
Standard Deviation (1 σ)	0.133 ft 0.041 m	0.071 ft 0.022 m	0.175 ft 0.053 m	0.119 ft 0.036 m
95 th Percentile	0.452 ft 0.138 m	0.152 ft 0.046 m	0.337 ft 0.102 m	0.231 ft 0.070m

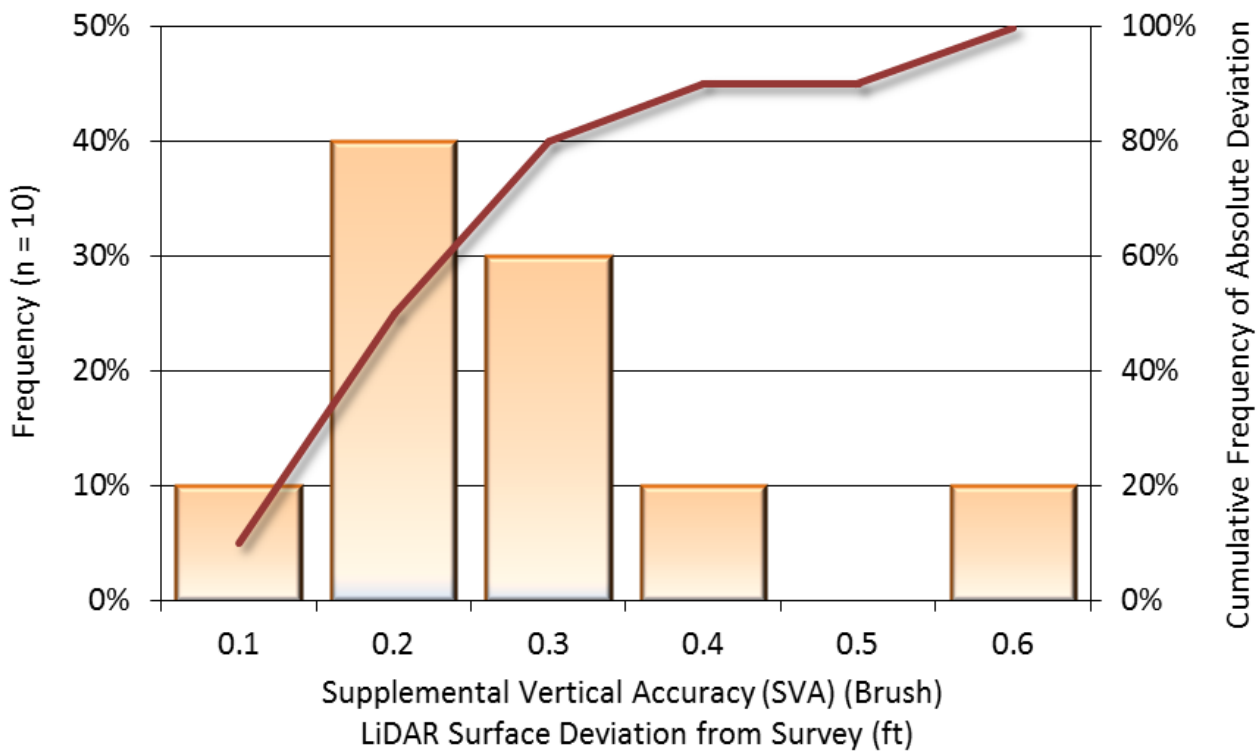


Figure 11: Frequency histogram for LiDAR surface deviation from “Brush” land cover class point values

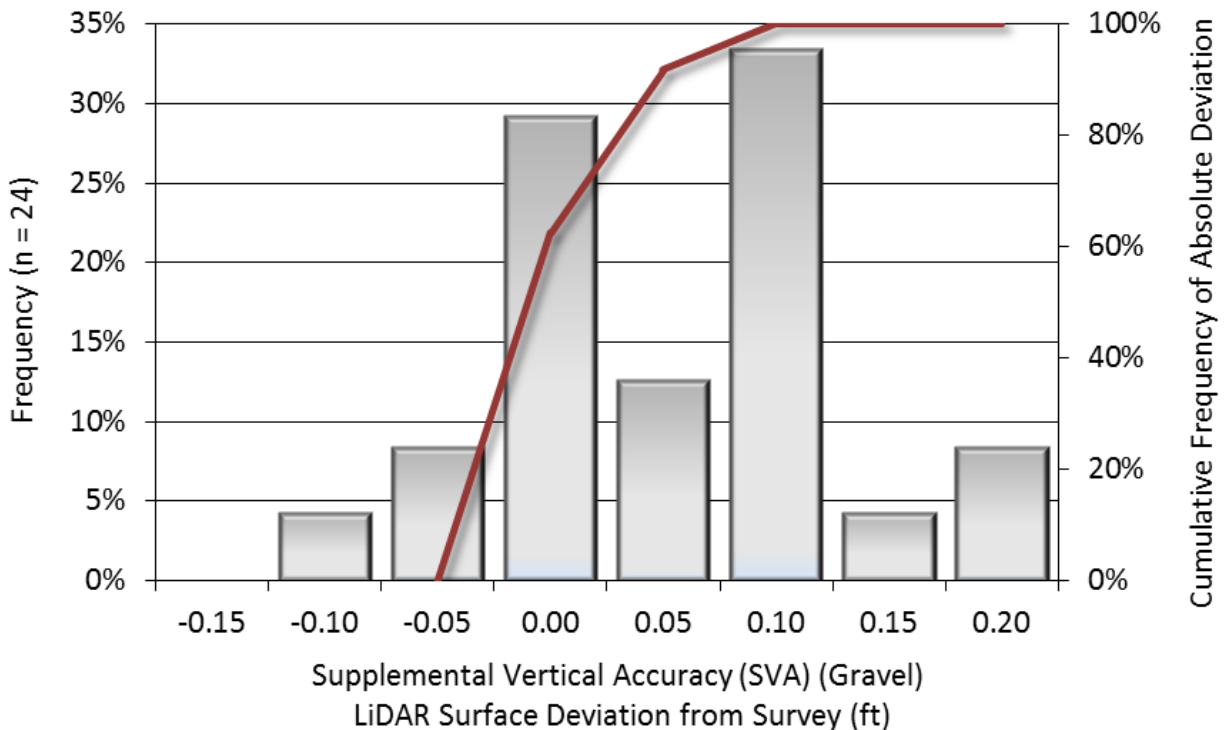


Figure 12: Frequency histogram for LiDAR surface deviation from “Gravel” land cover class point values

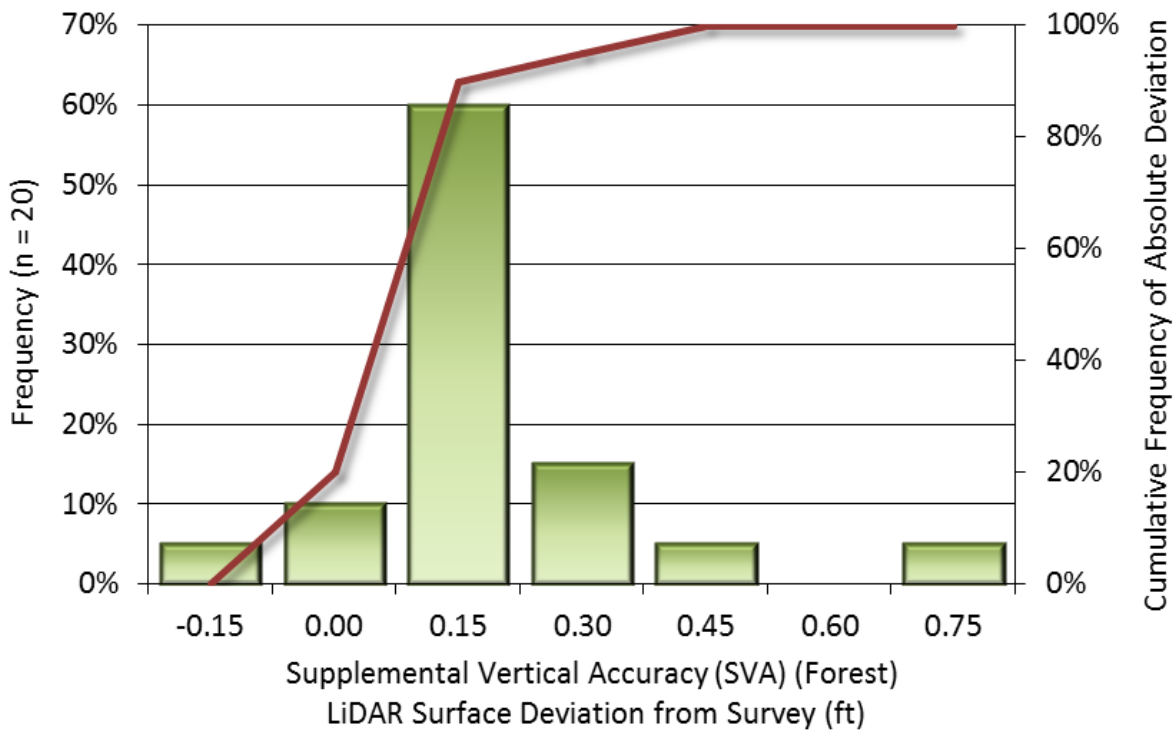


Figure 13: Frequency histogram for LiDAR surface deviation from “Forest” land cover class point values

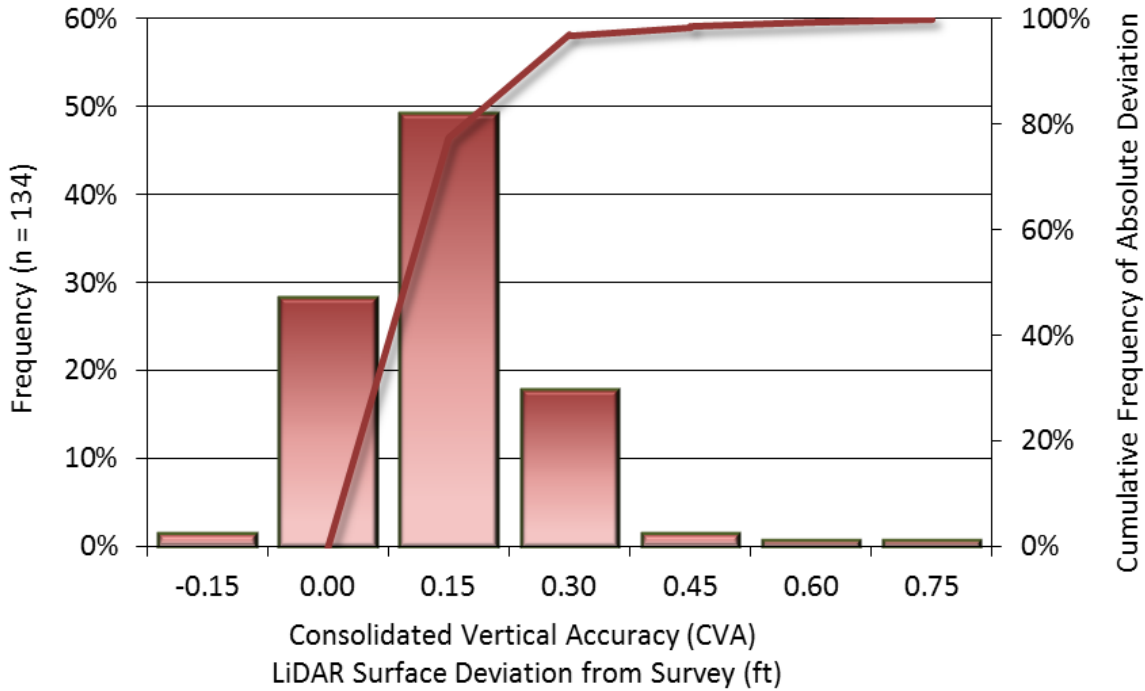


Figure 14: Frequency histogram for LiDAR surface deviation from all land cover class point values (CVA)

LiDAR Relative Vertical Accuracy

Relative vertical accuracy refers to the internal consistency of the data set as a whole: the ability to place an object in the same location given multiple flight lines, GPS conditions, and aircraft attitudes. When the LiDAR system is well calibrated, the swath-to-swath vertical divergence is low (<0.10 meters). The relative vertical accuracy was computed by comparing the ground surface model of each individual flight line with its neighbors in overlapping regions. The average (mean) line to line relative vertical accuracy for the Chena River Lakes LiDAR project was 0.114 feet (0.035 meters) (Table 11, Figure 15).

Table 11: Relative accuracy results

Relative Accuracy	
Sample	29 surfaces
Average	0.114 ft 0.035 m
Median	0.115 ft 0.035 m
RMSE	0.115 ft 0.035 m
Standard Deviation (1σ)	0.011 ft 0.003 m
1.96σ	0.022 ft 0.007 m

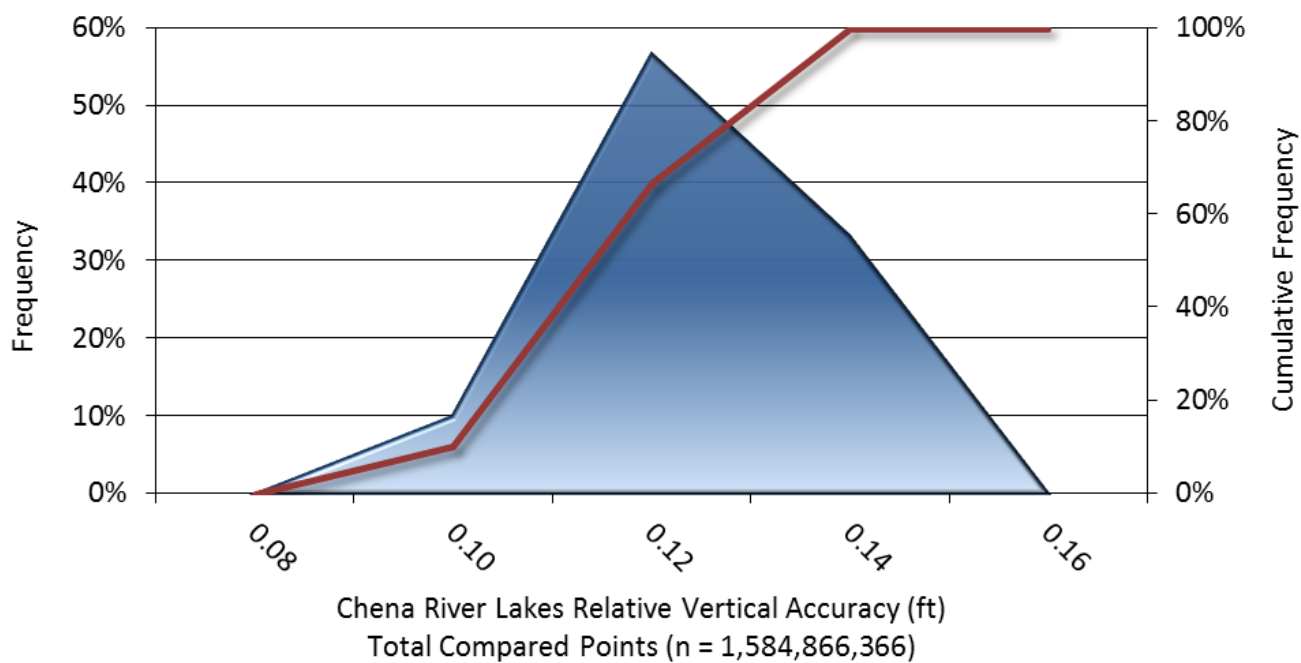


Figure 15: Frequency plot for relative vertical accuracy between flight lines

GLOSSARY

1-sigma (σ) Absolute Deviation: Value for which the data are within one standard deviation (approximately 68th percentile) of a normally distributed data set.

1.96 * RMSE Absolute Deviation: Value for which the data are within two standard deviations (approximately 95th percentile) of a normally distributed data set, based on the FGDC standards for Fundamental Vertical Accuracy (FVA) reporting.

Accuracy: The statistical comparison between known (surveyed) points and laser points. Typically measured as the standard deviation (sigma σ) and root mean square error (RMSE).

Absolute Accuracy: The vertical accuracy of LiDAR data is described as the mean and standard deviation (sigma σ) of divergence of LiDAR point coordinates from ground survey point coordinates. To provide a sense of the model predictive power of the dataset, the root mean square error (RMSE) for vertical accuracy is also provided. These statistics assume the error distributions for x, y and z are normally distributed, and thus we also consider the skew and kurtosis of distributions when evaluating error statistics.

Relative Accuracy: Relative accuracy refers to the internal consistency of the data set; i.e., the ability to place a laser point in the same location over multiple flight lines, GPS conditions and aircraft attitudes. Affected by system attitude offsets, scale and GPS/IMU drift, internal consistency is measured as the divergence between points from different flight lines within an overlapping area. Divergence is most apparent when flight lines are opposing. When the LiDAR system is well calibrated, the line-to-line divergence is low (<10 cm).

Root Mean Square Error (RMSE): A statistic used to approximate the difference between real-world points and the LiDAR points. It is calculated by squaring all the values, then taking the average of the squares and taking the square root of the average.

Data Density: A common measure of LiDAR resolution, measured as points per square meter.

Digital Elevation Model (DEM): File or database made from surveyed points, containing elevation points over a contiguous area. Digital terrain models (DTM) and digital surface models (DSM) are types of DEMs. DTMs consist solely of the bare earth surface (ground points), while DSMs include information about all surfaces, including vegetation and man-made structures.

Intensity Values: The peak power ratio of the laser return to the emitted laser, calculated as a function of surface reflectivity.

Nadir: A single point or locus of points on the surface of the earth directly below a sensor as it progresses along its flight line.

Overlap: The area shared between flight lines, typically measured in percent. 100% overlap is essential to ensure complete coverage and reduce laser shadows.

Pulse Rate (PR): The rate at which laser pulses are emitted from the sensor; typically measured in thousands of pulses per second (kHz).

Pulse Returns: For every laser pulse emitted, the number of wave forms (i.e., echos) reflected back to the sensor. Portions of the wave form that return first are the highest element in multi-tiered surfaces such as vegetation. Portions of the wave form that return last are the lowest element in multi-tiered surfaces.

Real-Time Kinematic (RTK) Survey: A type of surveying conducted with a GPS base station deployed over a known monument with a radio connection to a GPS rover. Both the base station and rover receive differential GPS data and the baseline correction is solved between the two. This type of ground survey is accurate to 1.5 cm or less.

Post-Processed Kinematic (PPK) Survey: GPS surveying is conducted with a GPS rover collecting concurrently with a GPS base station set up over a known monument. Differential corrections and precisions for the GNSS baselines are computed and applied after the fact during processing. This type of ground survey is accurate to 1.5 cm or less.

Scan Angle: The angle from nadir to the edge of the scan, measured in degrees. Laser point accuracy typically decreases as scan angles increase.

Native LiDAR Density: The number of pulses emitted by the LiDAR system, commonly expressed as pulses per square meter.

APPENDIX A - ACCURACY CONTROLS

Relative Accuracy Calibration Methodology:

Manual System Calibration: Calibration procedures for each mission require solving geometric relationships that relate measured swath-to-swath deviations to misalignments of system attitude parameters. Corrected scale, pitch, roll and heading offsets were calculated and applied to resolve misalignments. The raw divergence between lines was computed after the manual calibration was completed and reported for each survey area.

Automated Attitude Calibration: All data were tested and calibrated using TerraMatch automated sampling routines. Ground points were classified for each individual flight line and used for line-to-line testing. System misalignment offsets (pitch, roll and heading) and scale were solved for each individual mission and applied to respective mission datasets. The data from each mission were then blended when imported together to form the entire area of interest.

Automated Z Calibration: Ground points per line were used to calculate the vertical divergence between lines caused by vertical GPS drift. Automated Z calibration was the final step employed for relative accuracy calibration.

LiDAR accuracy error sources and solutions:

Type of Error	Source	Post Processing Solution
(Static/Kinematic)	Long Base Lines	None
	Poor Satellite Constellation	None
	Poor Antenna Visibility	Reduce Visibility Mask
Relative Accuracy	Poor System Calibration	Recalibrate IMU and sensor offsets/settings
	Inaccurate System	None
Laser Noise	Poor Laser Timing	None
	Poor Laser Reception	None
	Poor Laser Power	None
	Irregular Laser Shape	None

Operational measures taken to improve relative accuracy:

Low Flight Altitude: Terrain following was employed to maintain a constant above ground level (AGL). Laser horizontal errors are a function of flight altitude above ground (about 1/3000th AGL flight altitude).

Focus Laser Power at narrow beam footprint: A laser return must be received by the system above a power threshold to accurately record a measurement. The strength of the laser return (i.e., intensity) is a function of laser emission power, laser footprint, flight altitude and the reflectivity of the target. While surface reflectivity cannot be controlled, laser power can be increased and low flight altitudes can be maintained.

Reduced Scan Angle: Edge-of-scan data can become inaccurate. The scan angle was reduced to a maximum of $\pm 15^\circ$ from nadir, creating a narrow swath width and greatly reducing laser shadows from trees and buildings.

Quality GPS: Flights took place during optimal GPS conditions (e.g., 6 or more satellites and PDOP [Position Dilution of Precision] less than 3.0). Before each flight, the PDOP was determined for the survey day. During all flight times, a dual frequency DGPS base station recording at 1 second epochs was utilized and a maximum baseline length between the aircraft and the control points was less than 13 nm at all times.

Ground Survey: Ground survey point accuracy (<1.5 cm RMSE) occurs during optimal PDOP ranges and targets a minimal baseline distance of 4 miles between GPS rover and base. Robust statistics are, in part, a function of sample size (n) and distribution. Ground survey points are distributed to the extent possible throughout multiple flight lines and across the survey area.

50% Side-Lap (100% Overlap): Overlapping areas are optimized for relative accuracy testing. Laser shadowing is minimized to help increase target acquisition from multiple scan angles. Ideally, with a 50% side-lap, the nadir portion of one flight line coincides with the swath edge portion of overlapping flight lines. A minimum of 50% side-lap with terrain-followed acquisition prevents data gaps.

Opposing Flight Lines: All overlapping flight lines have opposing directions. Pitch, roll and heading errors are amplified by a factor of two relative to the adjacent flight line(s), making misalignments easier to detect and resolve.